Available online at www.sciencedirect.com
SCIENCE DIRECT®
ELSEVIER
Colloids and Surfaces A: Physicochem. Eng. Aspects 284–285 (2006) 548–551
COLLOIDS AND SURFACES A
www.elsevier.com/locate/colsurfa

# Effect of honeycomb film on protein adsorption, cell adhesion and proliferation

Hiroshi Sunami [a,*], Emiko Ito [b], Masaru Tanaka [a,b], Sadaaki Yamamoto [a,b], Masatsugu Shimomura [b,c]

[a] *Creative Research Initiative "Sousei" (CRIS), Hokkaido University, Hokkaido, Japan*
[b] *CREST, Japan Science and technology Corporation (JST), Japan*
[c] *Nanotechnology Research Center, Research Institute for Electronic Science, Hokkaido University, Hokkaido, Japan*

Received 1 November 2005; received in revised form 8 November 2005; accepted 10 November 2005
Available online 4 January 2006

**Abstract**

This article describes novel methods for controlling of cell adhesion by using micro porous polymer films. Recently we found the highly ordered micro porous films were formed when poly(ε-caprolactone) (PCL) solution was cast on substrates at high atmospheric humidity. The micro porous film has regular honeycomb morphology with a size of 5 μm per cell (honeycomb film). Endothelial cells grew rapidly on the honeycomb film. After 24 h cell culture, the cell number on honeycomb films was lager than that on PCL flat films. In order to elucidate the effect of honeycomb films as a scaffold for cell culture, the adsorbed proteins on honeycomb films under cell culture condition were observed. After conditioning of the honeycomb film and the flat film in DMEM containing 10% foetal bovine serum (FBS) for 72 h at 37 °C in 5% $CO_2$ atmosphere, the adsorbed fibronectin-FITC and albumin-Texasred on the honeycomb films was observed by using confocal laser scanning microscope (CLSM). The observation revealed that fibronectin showed site-selective adsorption behavior on the honeycomb film. Albumin adsorbed on the honeycomb film non site-selectively, while fibronectin mainly adsorbed on inside of honeycomb pores. On the flat film, fibronectin was hardly observed. Since the honeycomb film accelerate the adsorption of fibronectin which is a typical protein as a cell adhesion molecule, the film could be a scaffold with excellent cell adhesion properties.


*Keywords:* Honeycomb film; Cell adhesion; Cell proliferation; Fibronectin; Tissue engineering; Self-organization

## 1. Introduction

Cell behaviors such as growth, apoptosis and differentiation are controlled by micro-patterned cell adhesive surface [1–3]. Therefore, micro-patterning of cell adhesive regions attracts much attention. A large number of methods for preparing micro-patterned cell adhesive surface have been developed by photolithography and related techniques [1–18].

We have reported that micrometer size patterned polymer film (honeycomb film) can be prepared by self-organization [19]. The honeycomb film possessing a hexagonal array of micropores could be obtained by solution casting of various types of polymers on a solid substrate in a humid atmosphere. This method is simple and does not require special instrumentation in comparison with the photolithography method. Recently, we reported that honeycomb film could be utilized for the micropatterned cell culture substrate [20–22]. The honeycomb film can modulate cell adhesion and concomitant behavior such as morphological change and expression of cell function [23–26]. In order to elucidate the effect of honeycomb films as a scaffold for cell culture, the adsorbed proteins on honeycomb films under cell culture condition were observed. Since adsorption of proteins on substrates is thought to be an initial process for cell adhesion and growth, it is important to reveal the protein adsorption on honeycomb film. In this research, adsorbed proteins on honeycomb films were determined by immunostaining, and their topological structure were observed by confocal laser scanning microscopy.

## 2. Experiment

The honeycomb film was fabricated by applying a moist air to a spread polymer solution containing biodegradable

* Corresponding author. Tel.: +81 11 706 9255
*E-mail address:* sunami@poly.es.hokudai.ac.jp (H. Sunami).

0927-7757/$ – see front matter © 2005 Elsevier B.V. All rights reserved.
doi:10.1016/j.colsurfa.2005.11.041

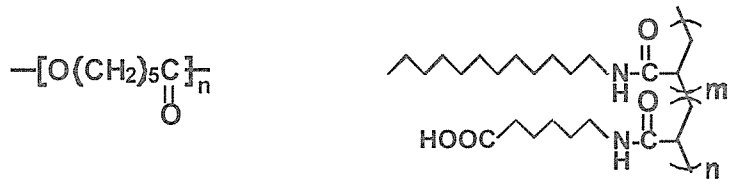


1 Poly( ε -caproractone)(PCL) 2 Amphiphilic polymer (CAP)

Scheme 1.

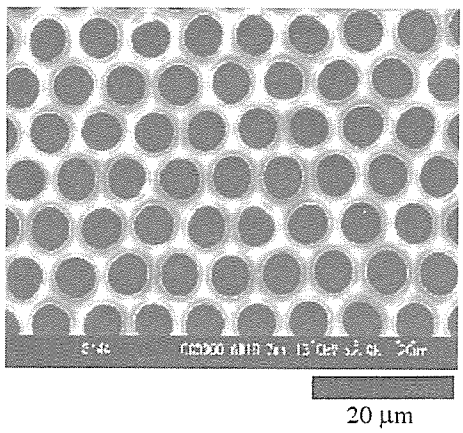


Fig. 1. SEM image of honeycomb film (PCL, pore size 5 μm).

polymers (poly(ε-caprolactone) (PCL)) 1 and an amphiphilic polymer (co-carboxyhexyl acrylamide (CAP)) 2 (10:1 wt.%) (Scheme 1). A chloroform solution (5 mg/ml) containing PCL (MW = 70,000–100,000) and CAP (MW = 20,000) were used. Evaporative cooling lead to the formation of hexagonally-packed water droplets on the polymer solution. The honeycomb structure with pore diameter of 5 μm and a wall thickness of 8 μm was prepared on disk-type cover grass (Ø 15 mm) (Fig. 1). Flat films made from the same materials, were prepared as a reference. These honeycomb films and flat films were immersed in 1-propanol for 12 min to remove the CAP.

After conditioning (pre-incubation) of the honeycomb films and the flat films in Dulbecco's modified Eagle's minimal essential medium (DMEM; SIGMA Co. Ltd, St. Louis, MO, USA) supplemented with 10% heat-inactivated fetal bovine serum (FBS; Thermo Trace Ltd., Melbourne, Australia) and 1% Penicillin–Streptomycin (Gibco, Grand Island, NY, USA) for 72 h at 37 °C in 5% $CO_2$ atmosphere, adsorbed fibronectin-FITC and albumin-Texas red on the honeycomb films was observed in PBS by using confocal laser scanning microscope (FV-300, Olympus. Co., Tokyo, Japan). Fibronectin and albumin in the FBS previously were immunostained by anti-fibronectin FITC conjugate (Biogenesis Ltd., UK) and anti-albumin Texas red conjugate (Rockland immunochemicals, Inc., USA).

Porcine aortic endothelial cells (ECs, passage 2) were purchased from DAINIPPON PHARMACEUTICAL Co., Ltd. The honeycomb films and the flat films were insert to 24-well plates (IWAKI Microplate; IWAKI Glass Co., Funahashi, Japan). The ECs were used at passage 6 to seed the 24-well plate at a concentration of $1.5 \times 10^4$ cells/cm$^2$ (cells/ml) in 1 ml DMEM supplemented with 10% FBS and 1% Penicilli–Streptomycin.

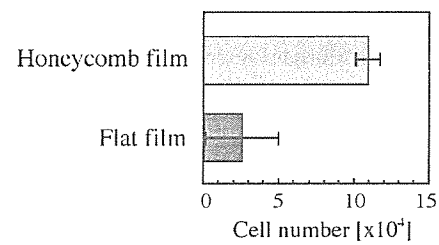


Fig. 3. Number of ECs on honeycomb film and on flat film after 24 h incubation.

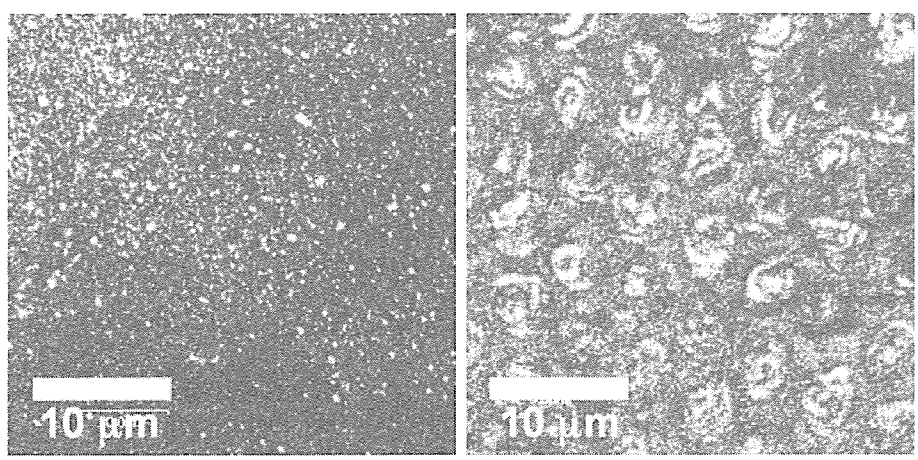


Fig. 2. Fluorescence images of adsorbed protein after 72 h conditioning on flat film and on honeycomb film. Green points are adsorbed fibronectin. Red points are adsorbed albumin.

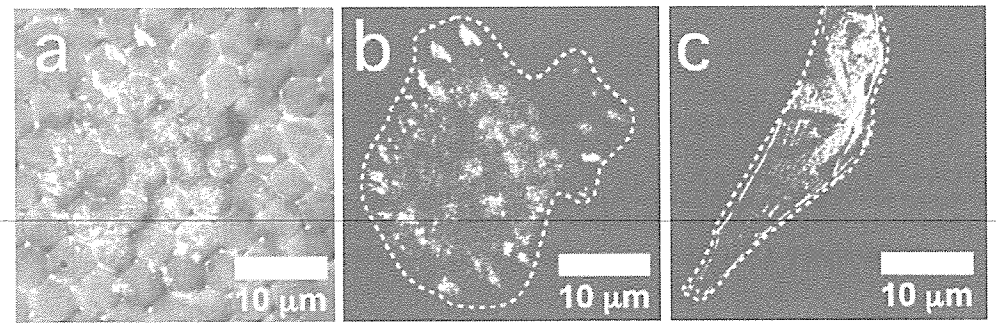


Fig. 4. (a) Superposition image between differential interference image of honeycomb film and immnostained vinculin of EC on the honeycomb film. Comparison of focal adhesion points of EC between on (b) honeycomb film and (c) flat film. White dots are outline of an EC. Red points are immnostained vinculin cluster (Alexa Fluor 546).

After 24 h the ECs culture, the number on the each substrate was evaluated with the Cell Proliferation Reagent WST-1 (F. Hoffmann-La Roche Ltd., Basel, Switzerland). All cell cultures were maintained in a humidified incubator at 37 °C in 5% $CO_2$/95% air.

After 24 h on the substrates, cells were washed with PBS and fixed with 10% formalin in PBS for 10 min. The cells were made permeable with 1% Triton-X for 30 min, washed with 0.05% T-PBS for 5 min, and incubated with a 1:100 dilution of mouse anti-vinculin monoclonal antibody (CHEMICON international, Inc., Temecula, CA, USA), respectively, for 90 min at 37 °C. After washed with 0.05% T-PBS for 5 min, the cells were labeled with a 1:1000 dilutions of Alexa Fluor 546 rabbit anti-goat IgG (Molecular Probes, Inc., Eugene, OR, USA) in PBS for 60 min at 37 °C. The cells were visualized with the confocal laser scanning microscope (FV-300, Olympus. Co., Tokyo, Japan).

## 3. Results and discussion

After 72 h conditioning, the fluorescence images of the adsorbed fibronectin-FITC and the albumin-Texas red on the honeycomb films and the flat films are shown in Fig. 2. The observation revealed that the fibronectins show characteristic adsorption behavior on the honeycomb film. However, the fibronectins (green points) hardly adsorbed on the flat films, the large amount of fibronectin adsorbed on the honeycomb film. Albumin (red points) adsorbed on the honeycomb film non site-selectively, while fibronectin mainly adsorbed on inside of honeycomb pores. It should be noted that clearly difference was observed for the adsorbed fibronectin structure between the honeycomb films and the flat films, although the surface chemical compositions are the same.

After 24 h incubation, the number of ECs on the honeycomb film was compared with that of ECs on the flat film (Fig. 3). The cell number on the honeycomb films was nearly four times lager than that on the flat films. The honeycomb film is expected to be a good scaffold for an EC culture system, because the honeycomb film could accelerate the EC proliferation.

The cell proliferation is highly regulated by cell-adhesion behavior onto biomaterials. Focal adhesion, which plays a crucial role in cell-adhesion behavior, is major cellular sites responsible for cell–protein attachment. The focal adhesion points (vinculin cluster) are mainly observed in inside of honeycomb pores (Fig. 4a). The site-selective distribution of focal adhesion points indicates that ECs adhere to adsorbed fibronectin molecules in the honeycomb pores. The morphology of focal adhesion points was clearly different between the honeycomb film (Fig. 4b) and the flat film (Fig. 4c), it was suggested that the difference of cell proliferation properties between these films is caused by the difference of focal adhesion points. The honeycomb film can control cell adhesion and proliferation by regulating the protein adsorption. This makes honeycomb film effective cell culture scaffold with high adhesion properties.

## 4. Conclusion

We reported that the site-selectively fibronectin adsorbed honeycomb film plays vital roles in cell adhesion and proliferation. The honeycomb film was demonstrated influencing cellular attachment and growth via the site-selective adsorption structure of fibronectin molecules. Hence, the honeycomb film could be an excellent scaffold with accelerating properties of cell adhesion and proliferation. These results indicate that a new method of controlling the protein adsorption, and, ultimately mediating cell adhesion and cell proliferation by using honeycomb film.

## Acknowledgements

We are grateful for the funding for this work provided by "Special Coordination Funds for Promoting Science and Technology" of Ministry of Education, Culture, Sports, Science and Technology, and CREST, Japan Science and technology Corporation (JST).

## References

[1] R. Singhvi, A. Kumar, G.P. Lopez, G.N. Stephanopoulos, D.I.C. Wang, G.M. Whitesides, D.E. Ingber, Science 264 (1994) 696.
[2] C.S. Chen, M. Mrksich, S. Huang, G.M. Whitesides, D.E. Ingber, Science 276 (1997) 1425.
[3] S.N. Bhatia, M.L. Yarmush, M. Toner, J. Biomed. Mater. Res. 34 (1997) 189.
[4] B. Lom, K.E. Healy, P.E. Hochberger, J. Neurosci. Methods 50 (1993) 385.

[5] D.V. Nicolau, T. Taguchi, H. Taniguchi, S. Yoshikawa, Langmuir 15 (1999) 3845.
[6] S.P.A. Fodor, J.L. Read, M.C. Pirrung, L. Stryer, A.T. Lu, D. Solas, Science 251 (1991) 767.
[7] D.J. Pritchard, H. Morgan, J.M. Cooper, Angew. Chem. Soc. 114 (1999) 4432.
[8] T. Matsuda, T. Sugawara, Langmuir 11 (1995) 2272.
[9] S.K. Bhatia, J.J. Hickman, F.S. Ligler, J. Am. Chem. Soc. 114 (1992) 4432.
[10] D.A. Stenger, J.H. Georger, C.S. Dulcey, J.J. Hickman, A.S. Rudolph, T.B. Nielsen, S.M. McCort, H.M. Calvert, J. Am. Chem. Soc. 114 (1992) 8435.
[11] C.S. Dulcey, J.H.J. Georger, V. Krauthamer, D.A. Stenger, T.L. Fare, J.M. Calvert, Science 252 (1991) 551.
[12] M. Matsuzawa, K. Umemura, D. Beyer, K. Sugioka, W. Knoll, Thin Solid Films 305 (1997) 74.
[13] J. Lahiri, E. Ostuni, G.M. Whitesides, Langmuir 15 (1999) 2055.
[14] L.A. Kung, L. Kam, J.S. Hovis, S.G. Boxer, Langmuir 16 (2000) 6773.
[15] A. Barnard, J.P. Penault, B. Michel, H.R. Bosshard, E. Delamarche, Adv. Mater. 12 (2000) 1067.
[16] M. Mrksich, G.M. Whitesides, Annu. Rev. Biophys. Biomol. Struct. 25 (1996) 55.
[17] S. Takayama, J.C. McDonald, E. Ostuni, M.N. Liang, P.J.A. Kents, R.F. Ismaginov, G.M. Whitesides, Proc. Natl. Acad. Sci. U.S.A. 96 (1999) 5545.
[18] E. Delamarche, A. Bernard, H. Schmid, B. Michel, H. Biebuyck, Science 276 (1997) 779.
[19] N. Maruyama, T. Koito, J. Nishida, T. Sawadaishi, X. Cieren, K. Ijiro, O. Karthaus, M. Shimomura, Thin Solid Films 327–329 (1998) 854.
[20] T. Nishikawa, J. Nishida, R. Ookura, S. Nishimura, S. Wada, T. Karino, M. Shimomura, Mater. Sci. Eng. C 8–9 (1999) 495.
[21] T. Nishikawa, J. Nishida, R. Ookura, S. Nishimura, S. Wada, T. Karino, M. Shimomura, Mater. Sci. Eng. C 10 (1999) 141–146.
[22] J. Nishida, K. Nishikawa, S.-I. Nishimura, S. Wada, T. Karino, T. Nishikawa, K. Ijiro, M. Shimomura, Polym. J. 34 (3) (2002) 166–174.
[23] K. Sato, M. Tanaka, M. Takebayashi, K. Nishikawa, M. Shimomura, Int. J. Nanosci. 1 (5&6) (2002) 689–693.
[24] M. Tanaka, M. Takebayashi, M. Miyama, J. Nishida, M. Shimomura, Bio-Med. Mater. Eng. 14 (2004) 439–446.
[25] A. Tsuruma, M. Tanaka, N. Fukushima, M. Shimomura, e-J. Surf. Sci. Nanotechnol. 3 (2005) 159–164.
[26] T. Nishikawa, J. Nishida, K. Nishikawa, R. Ookura, H. Ookubo, H. Kamachi, M. Matsushita, S. Todo, M. Shimomura, Stud. Surf. Sci. Catal. 132 (2001) 509–512.

# Electroless Plating of Honeycomb and Pincushion Polymer Films Prepared by Self-Organization

**Hiroshi Yabu, Yuji Hirai, and Masatsugu Shimomura**

Nanotechnology Research Center, Research Institute for Electronic Science, Hokkaido University, N21W10, Kita-ku, Sapporo, 001-0021, Japan, Frontier Research System, The Institute of Physical and Chemical Research (RIKEN Institute), 2-1, Hirosawa, Wako, Saitama, 351-0198, Japan, Core Research for Evolutional Science and Technology (CREST), Japan Science and Technology Agency (JST), 4-1-8, Hon-cho, Kawaguchi, Saitama, 332-0012, Japan, and Graduate School of Science, Hokkaido University, N10W8, Kita-ku, Sapporo, 060-0610, Japan

Langmuir®
The ACS Journal of Surfaces and Colloids

Reprinted from
Volume 22, Number 23, Pages 9760–9764

# Electroless Plating of Honeycomb and Pincushion Polymer Films Prepared by Self-Organization

Hiroshi Yabu,*,†,‡,§ Yuji Hirai,|| and Masatsugu Shimomura*,†,‡,§

*Nanotechnology Research Center, Research Institute for Electronic Science, Hokkaido University, N21W10, Kita-ku, Sapporo, 001-0021, Japan, Frontier Research System, The Institute of Physical and Chemical Research (RIKEN Institute), 2-1, Hirosawa, Wako, Saitama, 351-0198, Japan, Core Research for Evolutional Science and Technology (CREST), Japan Science and Technology Agency (JST), 4-1-8, Hon-cho, Kawaguchi, Saitama, 332-0012, Japan, and Graduate School of Science, Hokkaido University, N10W8, Kita-ku, Sapporo, 060-0610, Japan*

*Received July 28, 2006. In Final Form: September 7, 2006*

This report describes the fabrication and electroless plating of regular porous and pincushion-like polymer structures prepared by self-organization. Honeycomb-patterned films were prepared by simple casting of polymer solution under applied humid air and pincushion structures by peeling off the top layer of the former films. Silver-deposited honeycomb-patterned films and pincushion films were obtained by simple electroless plating of the respective original structures. XPS revealed Ag deposition on the honeycomb-patterned film. After thermal decomposition or solvent elution of the template polymer, unique metal mesoscopic structures were obtained.

## 1. Introduction

Because of their large refractive indices, high thermal and electrical conductivities, and mechanical and chemical stability, micro- and nanostructured metal materials are widely used in electronic and photonic devices. The topology and size scale of these materials are among the most significant factors in terms of their device applications. For example, regular arrays of tiny metal spikes (smaller than 100 nm) are suited for use as electrodes in field emission displays.[1] Photonic crystals having two- or three-dimensional periodic structures have been fabricated from metal or semiconductor materials to develop novel optical circuits.[2] Recently, exotic materials having negative refractive indices, so-called "left-handed metamaterials", have been prepared from structured metal materials having periodic patterns on the sub-wavelength scale.[3]

Lithography-based technologies, for example, photolithography, soft lithography,[4] and nanoimprint lithography,[5] are widely used to prepare metal micro- or nanostructures. These "top-down" type micro-fabrication technologies fundamentally consist of three basic processes involving photochemical reactions of resists, etching, and plating. Electroless plating is a widely used method for metallizing surfaces and is a purely chemical process of reducing metal ions on catalysts introduced onto surfaces by chemical adsorption, sputtering, or vapor deposition.[6] A major advantage of electroless plating is its applicability to a wide variety of materials including insulating surfaces such as glass, silicon oxide surfaces, and organic polymers, without the need for any electrical equipment. Thus, this technique is widely used in lithography and is called rapid prototyping. These metal micro- or nanostructures can be applied for many practical applications including regular porous metal materials, for use as photonic crystals, microreactors, separation filters, and so on, and have been prepared not only by the lithographic "top-down" method but also by "bottom-up" processes. Porous anodic alumina[7] and inverse opals[8] are typical templates used in electroless plating to form metal micro- and nanostructures. Here, this report describes another electroless plating template for fabricating regular porous metal structures.

It has previously been reported that honeycomb-like porous polymer films were formed by the simple casting of polymer solutions under humid conditions.[9] During solvent evaporation, water droplets condensed and were deposited on the solution surface due to evaporative cooling. These droplets packed regularly by lateral capillary forces between each water droplet and by convectional flow.[10] After complete evaporation of the solvent and water, a porous honeycomb-like structure was formed. By using this method, several kinds of functional materials have been developed, including superhydrophobic surfaces,[11] thermally stable microporous films,[12] and cell culture substrates.[13] Moreover, a variety of microstructures such as pincushions,[14] microrings, and microdots could be formed by simple peeling

* Corresponding author. Tel./Fax: +81-11-706-9369. E-mail: yabu@poly.es.hokudai.ac.jp (H.Y.); shimo@poly.es.hokudai.ac.jp (M.S.).
† Nanotechnology Research Center, Hokkaido University.
‡ RIKEN Institute.
§ CREST.
|| Graduate School of Science, Hokkaido University.

(1) Knapp, W.; Bishoff, L.; Teichert, J. *Vacuum* **2003**, *69*, 345−349.
(2) Yablonovitch, E. *Phys. Rev. Lett.* **1987**, *58*, 2059−2062.
(3) (a) Smith, D. R.; Pendry, J. B.; Wiltshire, M. C. K. *Science* **2004**, *305*, 788−792. (b) Soukoulis, C. M.; Kafesaki, M.; Economou, E. N. *Adv. Mater.* **2006**, *18*, 1941−1952.
(4) (a) Xia, Y.; Whitesides, G. M. *Angew. Chem., Int. Ed.* **1998**, *37*, 550−575. (b) Geissier, M.; Xia, Y. *Adv. Mater.* **2004**, *16*, 1249−1269.
(5) Chou, S. Y.; Krauss, P. R.; Renstrom, P. J. *Appl. Phys. Lett.* **1995**, *67*, 3114−3116.
(6) Li, J.; Shacham-Diamand, Y.; Mayer, J. W. *Mater. Sci. Rep.* **1992**, *9*, 1−51.
(7) Choi, J.; Sauer, G.; Nielsch, K.; Wehrspohn, R. B.; Gosele, U. *Chem. Mater.* **2003**, *15*, 776−779.
(8) (a) Juárez, B. H.; Rubio, S.; Sánchez-Dehesa, J.; López, C. *Adv. Mater.* **2002**, *14*, 1486−1490. (b) Juárez, B. H.; Ibisate, M.; Palacios, J. M.; López, C. *Adv. Mater.* **2003**, *15*, 319−323.
(9) Widawski, G.; Rawiso, M.; François, B. *Nature (London)* **1994**, *369*, 387−389.
(10) (a) Maruyama, N.; Koito, T.; Nishida, J.; Sawadaishi, T.; Cieren, X.; Ijiro, K.; Karthaus, O.; Shimomura, M. *Thin Solid Films* **1998**, *327−329*, 854−856. (b) Karthaus, O.; Maruyama, N.; Cieren, X.; Shimomura, M.; Hasegawa, H.; Hashimoto, T. *Langmuir* **2000**, *16*, 6071−6076.
(11) (a) Yabu, H.; Shimomura, M. *Chem. Mater.* **2005**, *17*, 5231−5234. (b) Yabu, H.; Shimomura, M. *Mol. Cryst. Liq. Cryst.* **2006**, *445*, 125−129. (c) Yabu, H.; Takebayashi, M.; Tanaka, M.; Shimomura, M. *Langmuir* **2005**, *21*, 3235−3237.
(12) (a) Yabu, H.; Tanaka, M.; Ijiro, K.; Shimomura, M. *Langmuir* **2003**, *19*, 6297−6300. (b) Yabu, H.; Kojima, M.; Tsubouchi, M.; Onoue, S.; Sugitani, M.; Shimomura, M. *Colloids Surf., A* **2006**, *284−285*, 254−256.

10.1021/la062228r CCC: $33.50 
Published on Web 10/14/2006

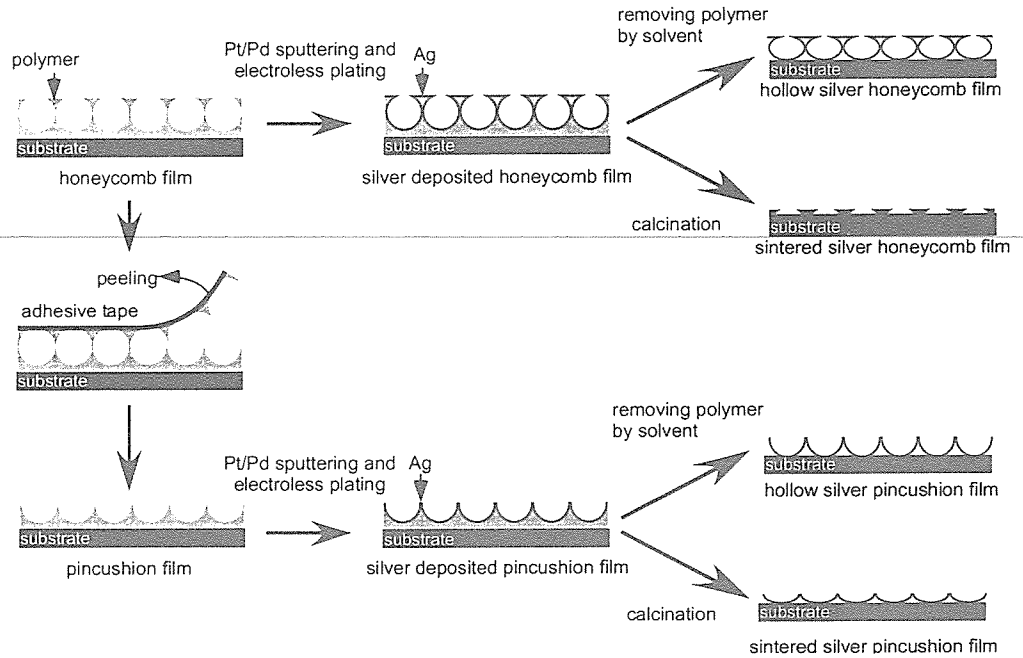


**Figure 1.** Schematic illustration of electroless plating, polymer elution, and calcination of self-organized honeycomb films and pincushion films.

Chart 1

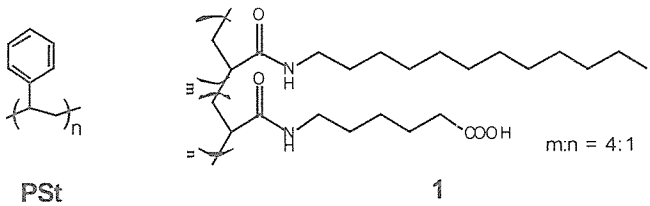


and thermal treatments. All of these textured substrates were basically organic polymer materials except for certain metal–alkoxide systems.[15] These microstructured films, therefore, had lower refractive indices, lower electrical conductivity, and lower chemical and mechanical stability than metal microstructures.

In this report, we show a simple fabrication method for fashioning honeycomb-patterned metal films by electroless plating (Figure 1). Metal pincushion structures were also prepared by simple peeling of the honeycomb-patterned polymer films and subsequent electroless plating. The polymer template was removed by sintering or solvent elution to complete the metallization. By these treatments, we obtained unique metallic structures by honeycomb and pincushion polymer films as templates.

## 2. Experimental Section

**2.1. Preparation of the Honeycomb-Patterned Films and Pincushion Films.** Honeycomb-patterned films were prepared by casting ca. 1.0–4.0 mg/mL chloroform solutions of polystyrene (Chart 1, PS, Aldrich, USA, $M_w$ ~280 000 g/mol) and amphiphilic copolymer **1** (Chart 1, PS:**1** = 9:1) in a 9 cm Petri dish. Polymer **1** was obtained by radical polymerization of 16.7 mmol of *N*-dodecylacrylamide (hydrophobic part) and 4.19 mmol of 6-acrylamidehexanoic acid (hydrophilic part) using 2.4 mmol of AIBN as an initiator in 84 mL of distilled benzene at 60 °C.[16] The product polymer was precipitated in acetonitrile, and then dried under vacuum pressure for 4 h. The yield of the polymer was 92%. The monomer unit ratio of hydrophobic part to hydrophilic part of the copolymer is ca. 4:1 as determined by C/N ratio of the elemental analysis. The molecular weight of the copolymer is $M_n$ = 33 000, $M_w$ = 250 000, $M_w/M_n$ = 7.6, which were measured by gel permeation chromatography (GPC, with using the Shodex column KF-804, Showadenko, Japan). The amphiphilic copolymer **1** stabilizes the condensed water droplets and prevents droplets from collapse. The casting volume varied from 1.0 to 10 mL. Moist air (temperature 23 °C, relative humidity ~90%) was applied vertically onto the solution surface at its velocity of 2.8 L/min. The diameter of the aperture used to apply moist air was 7 cm, and the distance between the solution surface and the aperature was ca. 12 cm. An opaque polymer film formed after evaporation of the chloroform solvent. The surface structure of the film was studied by optical microscopy (BH-2, Olympus, Japan), atomic force microscopy (AFM, SPI400, Seiko Instruments, Japan), and scanning electron microscopy (SEM, S-3500N, Hitachi, Japan). The pincushion film was prepared by peeling the surface off the honeycomb-patterned film with a sheet of adhesive tape (Scotch Tape, 3M, Japan).

**2.2. Electroless Plating of Honeycomb-Patterned Films and Pincushion Films.** Before electroless plating, the Pt/Pd catalyst used for electroless plating was sputtered onto the surface of a honeycomb-patterned or pincushion film for 50 s, depositing a ca. 10 nm thick Pt/Pd layer. After deposition of the catalyst layer, the film was soaked in an aqueous solution of silver nitrate. This solution contained 213 mg of silver nitrate (GR, Wako Chemical Industry, Japan) as the source of silver ion, 9.16 g of aqueous ammonia (28%, Wako Chemical Industry, Japan) and 2.16 g of acetic acid (GR, Wako Chemical Industry, Japan) to control pH, and 1.0 mL of hydrazine (GR, Wako Chemical Industry, Japan) as a reducer in 100 mL of water. After soaking for 1 to 5 min in the solution, the honeycomb-mesh film was rinsed twice with pure water. The film was dried at room temperature for 12 h and in vacuo for 2 h.

Elemental analysis of the surface before and after electroless plating was carried out by X-ray photoelectron spectroscopy (XPS, JPS-9200, JEOL, Japan). Al Kα X-rays with an energy of 1486.6 eV were used with a pass energy of 10 eV.

(13) (a) Nishikawa, T.; Nishida, J.; Ookura, R.; Nishimura, S.-I.; Wada, S.; Karino, T.; Shimomura, M. *Mater. Sci. Eng., C* **1999**, *10*, 141–146. (b) Nishikawa, T.; Nishida, J.; Ookura, R.; Nishimura, S.-I.; Wada, S.; Karino, T.; Shimomura, M. *Mater. Sci. Eng., C* **1999**, *8–9*, 495–500. (c) Nishikawa, T.; Ookura, R.; Nishida, J.; Arai, K.; Hayashi, J.; Kurono, N.; Sawadaishi, T.; Nishiura, Y.; Hara, M.; Shimomura, M. *Langmuir* **2002**, *18*, 5734–5740. (d) Nishikawa, T.; Nonomura, M.; Arai, K.; Hayashi, J.; Sawadaishi, T.; Nishiura, Y.; Hara, M.; Shimomura, M. *Langmuir* **2003**, *19*, 6193–6201.

(14) Yabu, H.; Shimomura, M. *Langmuir* **2006**, *22*, 4992–4997.

(15) (a) Karthaus, O.; Cieren, X.; Maruyama, N.; Shimomura, M. *Mater. Sci. Eng., C* **1999**, *10*, 103–106. (b) Yabu, H.; Shimomura, M. *Int. J. Nanosci.* **2002**, *1*, 673–676.

(16) Nishida, J.; Nishikawa, K.; Nishimura, S.-I.; Wada, S.; Karino, T.; Nishikawa, T.; Ijiro, K.; Shimomura, M. *Polym. J.* **2002**, *34*, 166–174.

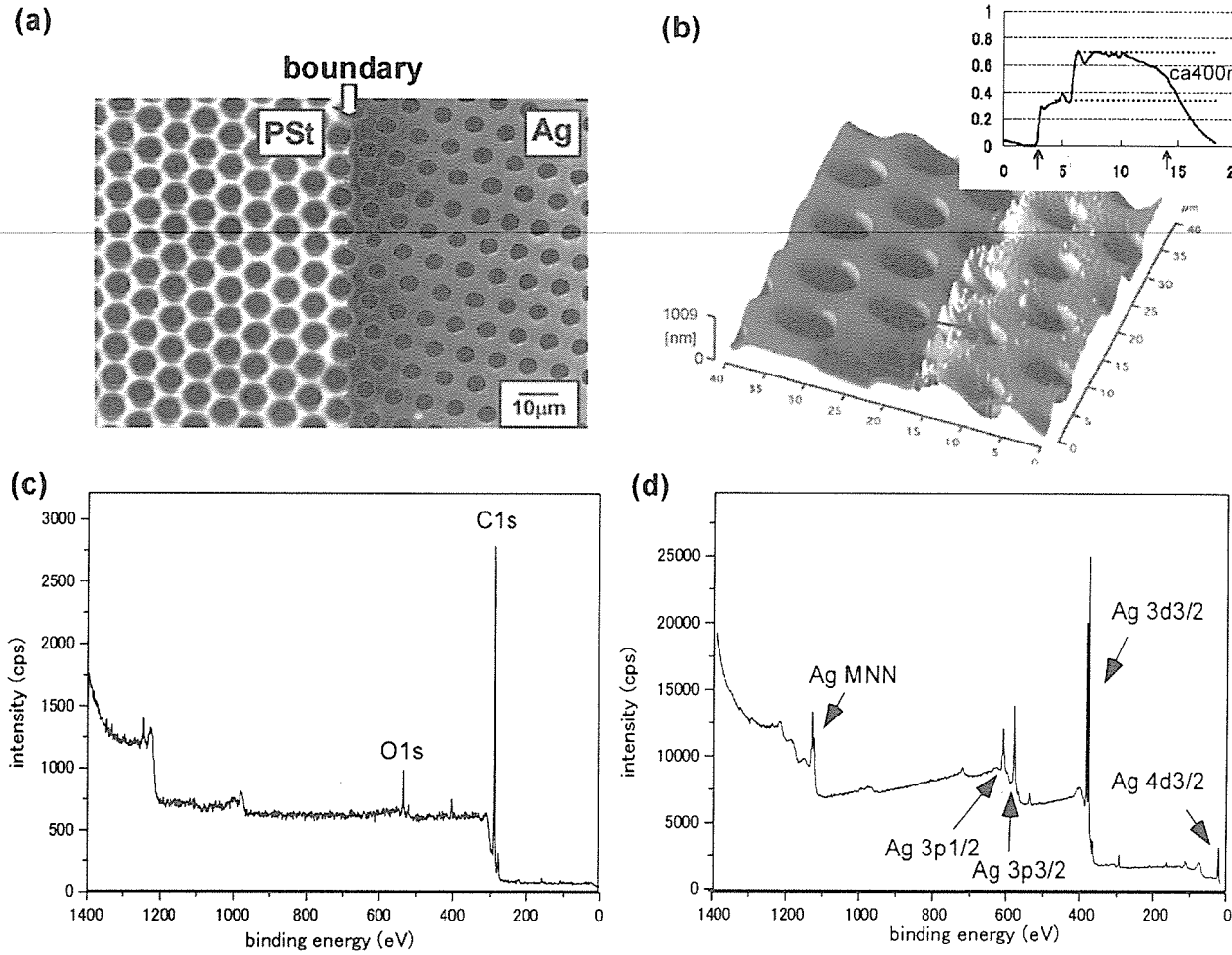


**Figure 2.** SEM (a) and AFM (b) images of silver deposited honeycomb films (inset of (b): cross-section of the AFM image). XPS spectra of the honeycomb mesh before (c)/after (d) deposition of silver. Platinum and palladium (Pt/Pd) were sputtered onto the prepared film for 50 s.

**2.3. Removal of Template by Elution or Sintering.** The films were immersed in chloroform for 2 h to wash out the template polymers, and sintered in an electric oven at ca. 200−400 °C for 2 h. The heating rate was 20 °C/min. After cooling to room temperature, the resulting metal structures without polymer templates were observed via SEM.

## 3. Results and Discussion

**3.1. Preparation and Metallization of Honeycomb-Patterned Polymer Films.** A solution of **1** and PS in chloroform was cast on a glass substrate. After complete evaporation of the solvent, a white translucent polymer film with interference colors was formed, having ordered, uniformly sized micropores. The pore size could be adjusted from 4 to 10 $\mu$m by changing the casting volume.[13] The solvent evaporation time, which was equal to the water condensation time, was the main factor controlling pore size in all cases. Larger amounts of casting solution required longer times for complete solvent evaporation, and the water droplets were larger.

Electroless plating was carried out on the honeycomb-patterned polymer films bearing Pt/Pd catalyst on their surfaces. Silver was deposited onto the Pt/Pd catalyst sites according to the following chemical reactions:

$$N_2H_4 + 4OH^- \rightarrow N_2 + 4H_2O + 4e^- \quad (1)$$

$$Ag(NH_3)_2^+ + e^- \rightarrow Ag + 2NH_3\,(\text{on Pt/Pd}) \quad (2)$$

Reaction 2 only proceeded in the presence of Pd/Pt, and silver was thus selectively deposited on the Pt/Pd surface. Figure 2a shows an SEM image of this film after electroless plating. Only the right half of the film was sputtered, but the whole film was immersed in the electroless deposition solution. The boundary between the bare and metallized regions was clearly seen, and the hexagonally arranged porous structure remained after metal deposition, although the pore size decreased after plating. Basically, the surface of the polystyrene is hydrophobic, but formation of Pt/Pd catalyst layer hydrophilized the surface. As the result, the plating solution penetrated into the pores and the metal layer was formed. An optical micrograph of metallized honeycomb-patterned film shows the structure was kept after plating (see Supporting Information).

Figure 2b shows an AFM image of the boundary between the bare polymer and metal-deposited regions. From the height profile of a cross-section of the boundary region (inset of Figure 2b), the thickness of the deposited metal layer was found to be ca. 400 nm when the film was immersed in the metal ion solution for 1 min. The thickness of this layer could be controlled by changing the immersion time and the concentration of silver nitrate. This thickness increased linearly up to ca. 800 nm when the deposition time increased (3 min) during immersion in the same plating solution. The thickness was also increased with increasing silver nitrate concentration.

Figure 2c and d shows wide-scan XPS spectra of the film before and after electroless plating, respectively. Before deposi-

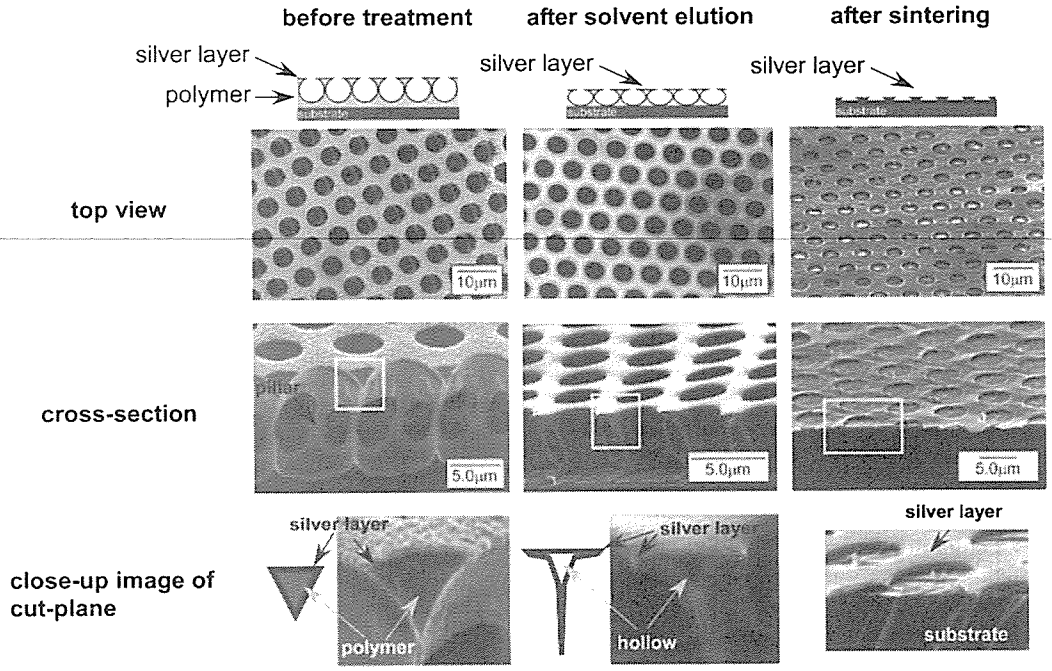


**Figure 3.** SEM images of silver deposited honeycomb-patterned films before/after solvent or heating treatment. Top view, cross-section, and close-up images of cut-plane (close-up regions are shown in the white squares) of each sample are shown.

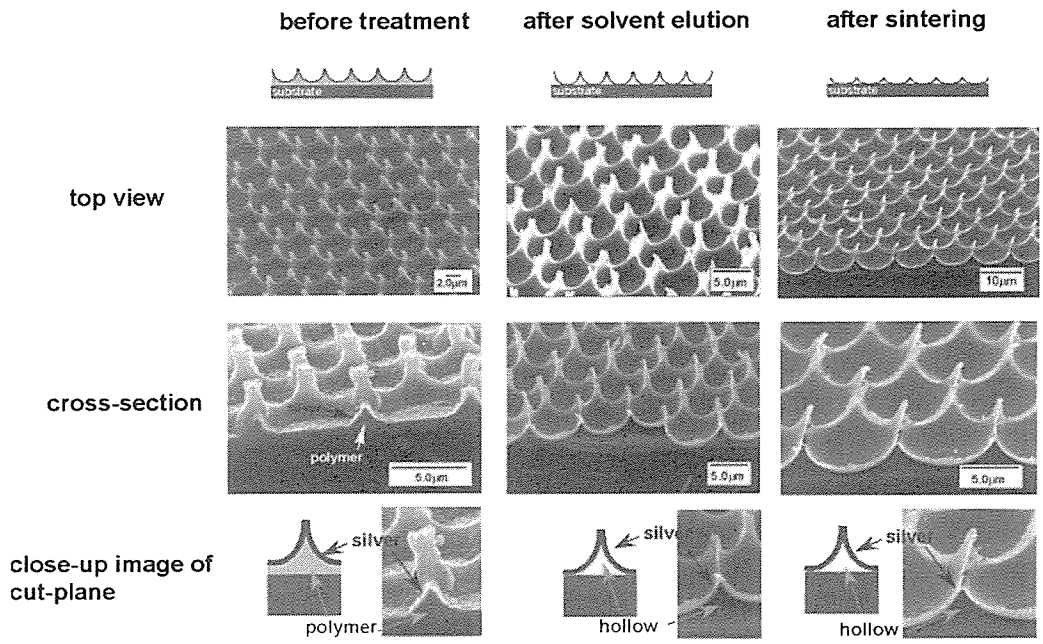


**Figure 4.** SEM image of silver deposited pincushion structure after solvent elution (a) and annealing (b). The close-up image of the upper image of (b) is shown in the bottom image.

tion, a single narrow peak attributed to C1s was clearly observed at 289 eV. This peak disappeared after the deposition, and concurrently several clear peaks emerged that could be attributed to elemental silver.[17] These results indicated that the surface of the honeycomb-patterned film was covered by elemental silver.

**3.2. Removal of Polymer from Ag-Deposited Honeycomb-Patterned Films by Solvent Elution or Thermal Decomposition.** The electroless plating technique that we mentioned above yielded polymer−metal hybrid honeycomb-patterned films. To make all-metal structures, the silver-deposited film was treated by the following two methods: immersion in solvent and sintering.

The left column in Figure 3 shows the surface and cross-section SEM images of these films. The cross-section showed the pillar structure supported by the bottom and top layers of the film, and the close-up image of the cut-plane showed a layer of silver covering the polymer template. The surface structure of the film remained almost unchanged after immersion in chloroform to dissolve the polymer template (top SEM image of center column in Figure 3). However, the cross-section image showed that the polymer was entirely removed, leaving a hollow silver frame (middle SEM image of center column in Figure 3). Thus, chloroform dissolved and removed the template polymer, leaving only a silver "skin". The cut-plane of the solvent-eluted film clearly showed that hollow spaces were formed in the silver skin layers (bottom SEM image of center column in Figure 3). The

(17) Ag specific photoelectron peaks including 3.03 eV (4d3/2), 366 eV (3d3/2), 572 eV (3p3/2), 602 eV (3p1/2), and 1132 eV (MNN) are observed. Each number shown after the binding energy is attributed to the orbitals of bulk Ag. The peak from MNN originated from the Auger electron of Ag.

thickness of the film decreased from ca. 10 to 6.5 $\mu$m after solvent elution. By contrast, after sintering for 2 h at 400 °C, which is above the decomposition temperature of PS, although the hexagonal periodicity was maintained (top SEM image of right column in Figure 3), the film thickness decreased by ca. 80% (middle SEM image of right column in Figure 3). This change in morphology was caused by breakdown of the pillars, which were mechanically weak because of the thinness of their centers. As a result, a thin, monolayered honeycomb-patterned silver structure remained after sintering.

**3.3. Preparation of Metal Pincushions and Removal of Template Polymer.** A pincushion-structured film could be prepared by peeling off the top layer of the honeycomb-patterned film with adhesive tape. The left column of Figure 4 shows SEM images of the pincushion structure after plating. Uniform, hexagonally arranged "spikes" of ca. 500 nm width remained on the film surface after plating.

The same two treatments just described were performed on these pincushion structures for polymer template removal. When the silver-deposited pincushion structure was immersed in chloroform, the surface structure was maintained (center column of Figure 4), but the tops of the spikes became narrower (middle and bottom images of center column of Figure 4). After the polymer was removed during elution, only the hollow spikes remained. The thickness decreased 200−400 nm after solvent elution. The silver layer on these spikes was too thin to maintain the mechanical integrity of these hollow structures, which collapsed upon elution of polymer. The same structure was formed after sintering the films at 400 °C for 2 h (right column of Figure 4). The polystyrene template was thermally degraded, forming a hollow space beneath the silver layer.

(18) Zhang, Y. S.; Yu, K.; Ouyang, S.; Zhu, Z. *Physica B* **2006**, *382*, 76−80.
(19) Wang, Z.; Rothberg, L. J. *Appl. Phys. B* **2006**, *84*, 289−293.
(20) Zhang, Z.; Yoshida, N.; Imae, T.; Xue, Q.; Bai, M.; Jiang, J.; Liu, Z. F. *J. Colloid Interface Sci.* **2001**, *243*, 382−387.

## 4. Conclusion

Honeycomb-patterned films were prepared by simple casting of polymer solution under applied humid air and pincushion structures by peeling off the top layer of the former films. Silver-deposited honeycomb-patterned films and pincushion films were obtained by simple electroless plating of the respective original structures. XPS revealed Ag deposition on the honeycomb-patterned film. After thermal decomposition or solvent elution of the template polymer, unique metal mesoscopic structures were obtained.

These periodic metal structures show good potential for a wide variety of practical applications. Periodic metal microporous structures could be used as two-dimensional photonic crystals based on their regularity and high refractive indices, or as microreactors because of their thermal and chemical stability. Transparent conductive films for flat panel displays are also a promising application. The metal pincushions could be used in field emission displays,[18] and as substrates for surface enhanced Raman scattering (SERS)[19] or surface-enhanced infrared absorption spectroscopy (SEIRAS) due to their small structures and high electrical conductivity.[20]

**Acknowledgment.** This work was partly supported by a Grant-in-Aid for Exploratory Research (No.16651074), a Grant-in-Aid for Scientific Research (A) (No.18201019), and a Grant-in-Aid for Young Scientists (A) (No.17681012), MEXT, Japan.

**Supporting Information Available:** An optical micrograph of the metallized honeycomb-patterned film. This material is available free of charge via the Internet at http://pubs.acs.org.

LA062228R

Available online at www.sciencedirect.com
ScienceDirect
Biomaterials 28 (2007) 1752–1760
Biomaterials
www.elsevier.com/locate/biomaterials

# Platelet adhesion to human umbilical vein endothelial cells cultured on anionic hydrogel scaffolds

Yong Mei Chen[a,d], Masaru Tanaka[b,d], Jian Ping Gong[a,e,*], Kazunori Yasuda[c,d], Sadaaki Yamamoto[d], Masatsugu Shimomura[b], Yoshihito Osada[a]

[a]*Graduate School of Science, Hokkaido University, Sapporo 060-0810, Japan*
[b]*Nanotechnology Research Center, Research Institute for Electronic Science, Hokkaido University, Sapporo 001-0021, Japan*
[c]*School of Medicine, Hokkaido University, Sapporo 060-0810, Japan*
[d]*Creative Research Initiative 'Sousei', Hokkaido University, Sapporo 001-0021, Japan*
[e]*SORST, JST, Sapporo 060-0810, Japan*

Received 17 August 2006; accepted 1 December 2006
Available online 22 December 2006

**Abstract**

In this work we describe experiments designed to understand the human platelet adhesion to human umbilical vein endothelial cells (HUVECs) cultured on various kinds of chemically cross-linked anionic hydrogels, which were synthesized by radical polymerization. HUVECs could proliferate to sub-confluent or confluent on poly(acrylic acid) (PAA), poly(2-acrylamido-2-methyl-propane sulfonic acid sodium salt) (PNaAMPS), and poly(sodium *p*-styrene sulfonate) (PNaSS) gels. The proliferation behavior was not sensitive to the cross-linker concentration of the gels. However, the platelet adhesion on the HUVECs cultured on these gels showed different behavior, as revealed by human platelet adhesion test in static conditions. Only a few platelets adhered on the HUVEC sheets cultured on PNaAMPS gels with 4 and 10 mol% cross-linker concentrations, and completely no platelet adhered on the HUVEC sheets cultured on PNaSS gels with 4 and 10 mol% cross-linker concentrations. On the other hand, a large number of platelets adhered on the HUVECs cultured on PAA gels with 1, 2 mol% cross-linker concentrations and PNaAMPS gel with 2 mol% cross-linker concentration. Furthermore, the study showed that promote of the glycocalyx of HUVECs with transforming growth factor-$\beta_1$ (TGF-$\beta_1$) decreased platelet adhesion, and degrade the glycocalyx with heparinase I increased platelet adhesion. The results suggested that the glycocalyx of cultured HUVECs modulates platelet compatibility, and the amount of glycocalyx secreted by HUVECs dependents on the chemical structure and cross-linker concentration of gel scaffolds. This result should be applied to make the hybrid artificial blood vessel composes of gels and endothelial cells with high platelet compatibility.


*Keywords:* Platelet adhesion; Hydrogel; Cell culture; Glycocalyx

## 1. Introduction

Blood compatibility is one of the basic required parameters of biomaterials, which is suitable for application as artificial blood vessel. It is well-known that the major problem of the artificial blood vessel is that blood clot occurs after a certain period of implantation, especially when the diameter of artificial blood vessel is smaller than 5 mm [1]. During the past decades, many studies have performed to understand the interaction of platelets with synthetic polymers, hoping to find materials that are compatible with the vascular system [2–9]. It has been shown that polymer surfaces modified by grafted polymers or anti-thrombogenic mediators reduce platelet adhesion [10–15]. However, blood compatibility of the modified polymers decreases with blood contacting time due to desquamation of the modified materials.

In the in vivo vascular systems, the inner surface of blood vessel is covered by a functional endothelial cell (EC)

*Corresponding author. Graduate School of Science, Hokkaido University, Sapporo 060-0810, Japan. Tel.: +81 11 706 2774; fax: +81 11 706 2774.
*E-mail address:* gong@sci.hokudai.ac.jp (J.P. Gong).

0142-9612/$ - see front matter © 2006 Elsevier Ltd. All rights reserved.
doi:10.1016/j.biomaterials.2006.12.005

monolayer which protects procoagulant activity. The EC surface is covered by a layer of glycocalyx of 0.5–3 μm in thickness [16], containing a large amount of proteoglycans (PGs). The main component of PGs is heparan sulfate PGs (HSPGs) (50–90%), which consist of core protein and heparan sulfate-type glycosaminoglycan [17,18]. It was reported that two kinds of HSPGs, prelecan and biglycan, exhibit antithrombin activity [19–21]. Prelecan actives antithrombin III by heparin-like sequences in the heparin sulfate chains, and biglycan actives heparin cofactor II by the dermatan sulfate chains. Perlecan-expressing cells completely prevent occlusive thrombosis, while injured arterial segments containing perlecan-deficient cells has a 23% thrombotic occlusion rate [22]. The study showed that transforming growth factor $\beta_1$ (TGF-$\beta_1$) can promote the synthesis of HSPGs when EC density is high [23]. On the other hand, heparinase can degrade HSPGs [24].

The ideal artificial blood vessel should have the structure similar to in vivo blood vessel and take full advantages of cell functions. Therefore, artificial blood vessel with EC monolayer on its inner wall has been expected to inhibit thrombosis. However, the blood compatibility of in vitro cultured ECs is poorly investigated [25]. It is doubtful that the in vitro cultured ECs have the same anti-thrombogenic function as that of ECs in vivo [26].

Hydrogels are expected as scaffolds for repairing and regenerating a wide variety of tissues and organs, due to their three-dimensional network structure and viscoelasticity, which are similar to the macromolecular-based extracellular matrix (ECM) in biological tissues [27,28]. We have found that bovine fetal aorta ECs (BFAECs) can spread, proliferate, and reach confluent on synthetic hydrogels with negative charges, such as poly(acrylic acid) (PAA), poly(2-acrylamido-2-methyl-propane sulfonic acid sodium salt) (PNaAMPS), and poly(sodium *p*-styrene sulfonate) (PNaSS), without surface modification with any cell adhesive proteins or peptides [29]. However, the platelet adhesion behavior of the ECs cultured on the gels is unclear.

In this work, we describe experiments designed to understand the human platelet adhesion to human umbilical vein ECs (HUVECs) cultured on various kinds of chemically cross-linked anionic hydrogels (Fig. 1). It was found that the platelet adhesion on the cultured HUVECs strongly dependents on the chemical structure and cross-linker concentration of hydrogels, and these results are associated with the amount of glycocalyx on the cultured HUVECs.

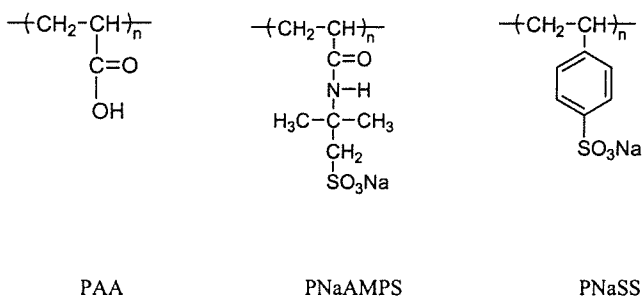


Fig. 1. Molecular structures of the polymers used in this work.

## 2. Materials and methods

### 2.1. Materials

2-Acrylamido-2-methyl-propane sulfonic acid sodium salt (NaAMPS) was obtained by neutralization of 2-acrylamido-2-methyl-propane sulfonic acid (Tokyo Kasei Kogyo, Tokyo, Japan) with sodium hydroxide in ethanol, and purified by recrystallization from acetone. Sodium *p*-styrene sulfonate (NaSS) and *N,N'*-methylenebis-(acrylamide) (MBAA) (Tokyo Kasei Kogyo, Tokyo, Japan) were purified by recrystallization from ethanol. Acrylic acid (AA) (Kanto Chemicals, Tokyo, Japan) was distilled at a reduced pressure. 2-Oxoglutaric acid (Wako Pure Chemicals, Osaka, Japan), sodium chloride, and sodium hydrogen carboxyl (Junsei chemicals, Tokyo, Japan) were used as purchased.

### 2.2. Hydrogel preparation

Hydrogels were synthesized and prepared as previously described [29]. Sheet-shaped gels were synthesized in the reaction cells that were formed by two parallel glass plates and separated by a silicone spacer of 1.5 mm thickness. An aqueous solution of 1 M monomer (AA, NaAMPS, or NaSS), 1–10 mol% cross-linker (MBAA), and 0.1 mol% initiator (2-oxoglutaric acid), was filled into the reaction cells. After being purged with nitrogen gas for 30 min, the cells were irradiated with UV light for polymerization (6 h).

After polymerization, gels were separated from the glass plates and immersed in a large amount of ion-exchanged water for 1 week. Water was changed two times every day to remove un-reacted residual chemicals. The gels were then immersed in 4-(2-hydroxyethyl) piperazine-1-ethanesulfonic acid sodium salt (HEPES) (Sigma, St. Louis, MO) buffer solution (HEPES $5 \times 10^{-3}$ M, $NaHCO_3$ $1.55 \times 10^{-2}$ M, NaCl 0.14 M, pH = 7.4). Phenol red ($2.5 \times 10^{-3}$ g/l) (Sigma, St. Louis, MO) was used to visualize the pH of the gels. After reaching equilibrium, the pH and ionic strength of solution containing in the gels was adjusted to 7.4 and c.a. 0.15 M, respectively. The thickness of equilibrated gels was about 2–3 mm. After sterilized by autoclaving (120 °C, 20 min), gel disks were punched out of the gel plates by a hole-punch with a radius of 1.5 cm. Then the gel disks were placed in a 24-well polystyrene (PS) tissue culture dish for HUVEC culture.

### 2.3. HUVEC culture

HUVECs (KURSBO Biomed. Bus., Tokyo, Japan) were cultured in Humedia-EB2 medium (KURSBO Biomed. Bus., Tokyo, Japan) containing 20% (v/v) fetal bovine serum (FBS) (GIBCO BRL Life Technologies, Inc., Gaithersburg, MD). $2.26 \times 10^4$ cells/cm$^2$ HUVEC suspension was seeded on the gel surfaces. The HUVECs-loading samples were cultured at 37 °C in a humidified atmosphere of 5% $CO_2$. The medium was changed every 24 h without damaging the HUVECs and the gels.

Floating HUVECs was counted with a haemocytometer at 6 h after seeding for determining the attached HUVEC number. The HUVEC morphology and proliferation on the gel surfaces were monitored using an Olympus IX 71 phase contrast microscope (Olympus, Japan) equipped with a digital camera using 10 × objective. The HUVEC monitoring was first performed at 6 h, and then monitored every 24 h, until the HUVECs proliferated to sub-confluent or confluent. HUVEC number counting was performed using the photography. More than four independent experiment runs were performed for each kind of gel. On each sample, four different areas were selected.

### 2.4. HSPGs modulation

TGF-$\beta_1$ (R&D Systems Inc., USA), which stimulates the HSPGs synthesis, was used to promote the amount of HSPGs on HUVEC surfaces [23,30]. Heparinase I (Sigma, St. Louis, MO), which cleaves heparin and heparin sulfate of HSPGs, was used to decrease the amount of HSPGs on HUVEC surfaces [31–33]. After proliferating to sub-confluent or confluent, HUVECs were incubated in 1 ml of 20 ng/ml TGF-$\beta_1$, which in serum containing medium, for 48 h, or 1 ml of 1.45 U/ml heparinase I, which in no serum containing medium, for 4 h.

### 2.5. Platelet adhesion test

Platelet adhesion test was performed in static conditions as previously described [3,4]. Human whole blood was drawn from healthy volunteer and mixed with a 1/9 volume of 3.8% sodium citrate. The blood was centrifuged at 1200 rpm for 5 min at room temperature for obtaining platelet-rich plasma (PRP). Then the residue was centrifuged at 3500 rpm for 10 min for obtaining platelet-poor plasma (PPP). The platelet concentration was determined by haemocytometer. The platelet density was adjusted to $1 \times 10^5$ cells/μl by mixing PRP and PPP. Then 200 μl (platelet number: $2 \times 10^7$) of the platelet suspension was loaded on the HUVECs proliferated to sub-confluent or confluent on PAA, PNaAMPS, and PNaSS gels, respectively, and incubated for 2 h at 37 °C. The bare poly(ethylene terephthalate) (PET) and PS plate, as well as the HUVECs proliferated to confluent on the PS plate were used as references. Hereafter, the HUVECs proliferated to confluent on the scaffolds is referred as HUVEC sheet.

After rinsing the weakly adhered platelets three times with phosphate buffer saline (PBS) (pH 7.4), adhered platelets were fixed by immersing the samples into 2.5 wt% glutaraldehyde of PBS for 2 h at 37 °C. Then the fixed samples were rinsed with PBS, 50% PBS, and ion-exchanged water. Samples were freeze-dried, and sputter-coated using a Pt–Pd target (E-1030, HITACHI) prior to observation by scanning electron microscope (SEM) (S-3500N, HITACHI). By counting the number of adhered platelets on the sample surfaces, the platelet adhesion densities were determined. More than three independent experimental runs were preformed for each kind of sample. On each sample, five different areas were selected.

### 2.6. Sample dehydration

For observing platelet morphology and counting the number of adhered platelets on cultured HUVECs by SEM, platelets, HUVECs, and the gels should be dehydrated without shape distortion. The conventional method to dehydrate the adhered platelets on the polymer modified solid scaffolds is not suitable for dehydrating the gel scaffolds with HUVECs and platelets [34]. Because in the process of conventional dehydration method, samples were treated by gradually exchanging solvent with ethanol/distilled water mixture (50–100% ethanol, 10% increment) before freeze drying. The process results in dramatic shrinkage of the gels, and most of the adhered platelets and HUVECs were exfoliated from the gel surfaces.

We solved this problem by the secondary freeze-drying operation (AdVantage Freeze Dryer Instruction, VIRTIS, Gardiner, USA). The process is as follow: after the temperature of freeze-drying chamber was decreased to −70 °C, the samples were put into the freeze-drying chamber and frozen at −70 °C for 2 h. The frozen samples were subsequently dehydrated at −40 °C for 5 h, −25 °C for 4 h, and 25 °C for 4 h. The vacuum was maintained at higher than 100 mTorr during the freeze-drying run. After the secondary freeze-drying, the size of the gels did not significantly changed, adhered platelets and HUVECs remained on the gel surfaces, keeping their original shapes.

## 3. Results and discussion

### 3.1. HUVECs growth on hydrogels

Cultivation of HUVECs on PAA, PNaAMPS, and PNaSS gels were performed. The gels were not modified with any cell adhesive proteins or peptides before HUVEC cultivation. The phase contrast micrographs of the HUVECs cultured on the PAA, PNaAMPS, and PNaSS gels, as well as on the reference, PS plate, at 144 h are shown in Fig. 2. The corresponding HUVEC densities on these scaffolds are shown in Fig. 3. HUVECs proliferate to confluent on the strong anionic gels, PNaAMPS (cross-linker conc. 2, 4, 10 mol%) and PNaSS (4, 10 mol%) at 144 h, with a cell density higher than $1.1 \times 10^5$ cell/cm$^2$, closed to that on PS plate. On the other hand, HUVECs proliferated to sub-confluent on the weak anionic PAA (1, 2 mol%) gel with a cell density of about $4.5 \times 10^4$ cell/cm$^2$.

Fig. 4 shows the HUVECs densities on PAA (1, 2 mol%), PNaAMPS (4 mol%), and PNaSS (10 mol%) gels, as well as on PS plate, as a function of culture time. HUVEC proliferation rates on 2 and 10 mol% PNaAMPS gels were the same as that on the 4 mol% PNaAMPS gel, and the cell proliferation rate on the 4 mol% PNaSS gel was the same as that on the 10 mol% PNaSS gel (data are not shown). It shows that the HUVEC proliferation rate on various scaffolds increases in the order of PAA $<$PNaAMPS$\approx$PNaSS$\approx$PS. In addition, the HUVEC proliferation rate is not dependent on the cross-linker concentration of the gels. The results are in agreement with our previous study on BFAECs cultured on PAA, PNaAMPS, and PNaSS gels, indicating that the ECs proliferation rate correlates with the charge density of negative charged gels [29].

### 3.2. Platelet adhesion on the HUVECs cultured on hydrogels

PET plate that is often used as a negative control scaffold of platelet adhesion [35,36], and PS plate that is often used as a cultivation scaffold of anchorage-dependent cells [37], were chosen as references for platelet adhesion test. The morphology of the adhered platelets (spherical shape, spreading shape, and pseudopodia extension) observed by SEM images is one of the indexes expressing the degree of the platelet activation [3–5]. SEM images of the adhered platelets on the HUVEC sheets cultured on various gels, and on the references, i.e. bare PET, PS, and the HUVEC sheet cultured on the PS, are shown in Fig. 5, the corresponding densities of adhered platelets on these samples are shown in Fig. 6.

Figs. 5 and 6 show that a large amount of platelets adhere on the bare PET plate (271 cells/$10^4$ μm$^2$), and 53.9% of all adhered platelets are spreading, 43.1% platelets are rounded with pseudopodia extension, indicating the activation of the platelets. Except on the bare PET plate, the platelets that adhere on the cultured HUVECs

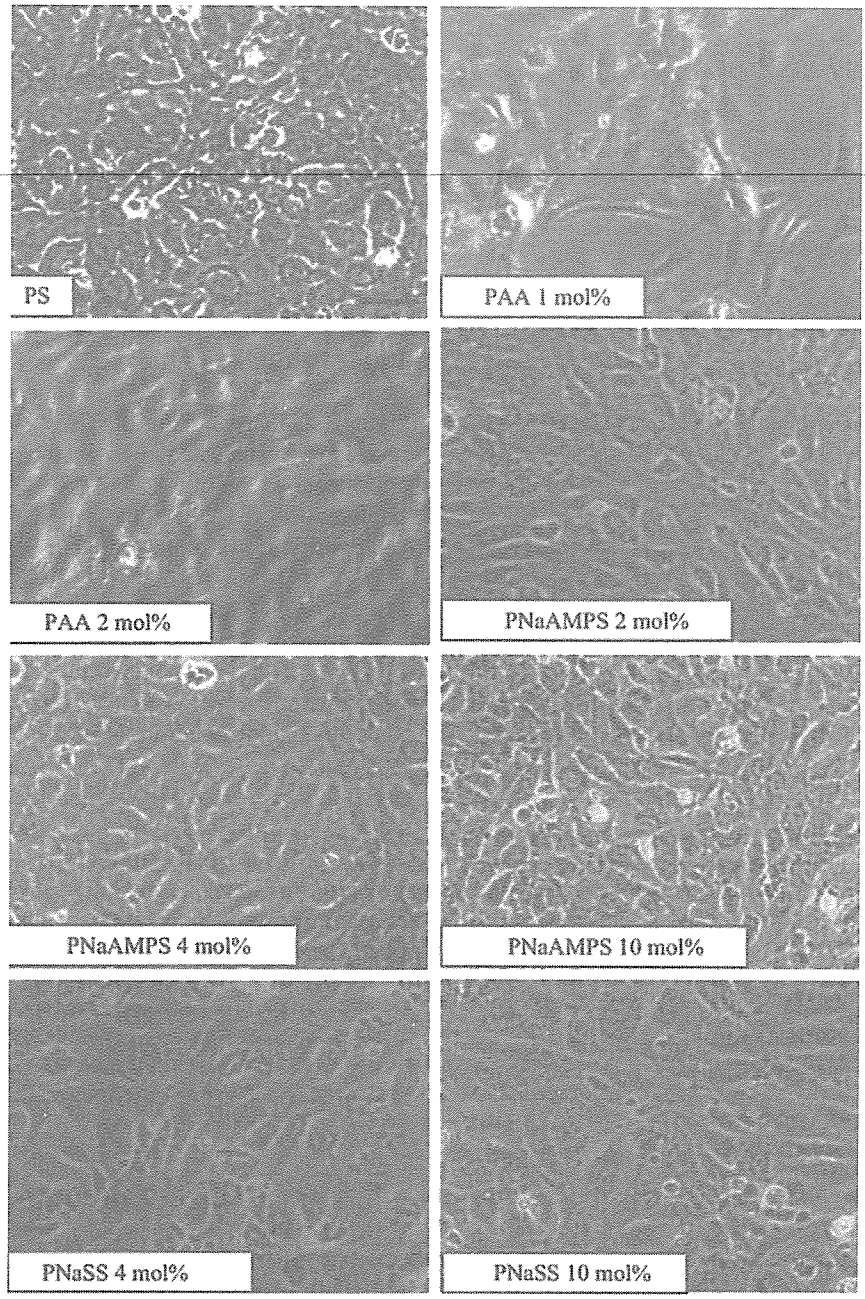


Fig. 2. Phase-contrast micrographs of the HUVECs cultured on various kinds of substrates at 144 h. The numbers in the figures are the concentration of MBAA in molar ratio in relative to monomer used in gelation. Scale bar: 100 μm.

and on the bare PS plate keep their original spherical shape, indicating not activate of the platelets. The density of adhered platelets on the HUVEC sheet cultured on the PS plate (185 cells/$10^4$ μm$^2$) is obviously lower than that on the bare PS plate (320 cells/$10^4$ μm$^2$). It shows that the HUVEC sheet cultured on the PS plate inhibits platelet adhesion comparing with the bare PS plate.

The platelets showed a similar adhesion behavior on the HUVECs cultured on the weak anionic PAA gels, and platelet adhesion on the HUVECs cultured on the PAA gels is not dependents on the cross-linker concentration of the gel. The density of adhered platelets on the as-prepared HUVECs cultured on PAA gels is 115 cells/$10^4$ μm$^2$. It should be noted that the HUVECs proliferate to sub-confluent on PAA gels, therefore, when the platelet suspension was cast on the HUVECs cultured on PAA gel, platelets could adhere on both of the HUVECs surface and on the PAA gel surface where no HUVECs exist. We can clearly distinguish the adhered platelets on the HUVECs surface from the adhered platelets on the PAA gel surface where no HUVECs exist by SEM images (Fig. 5).

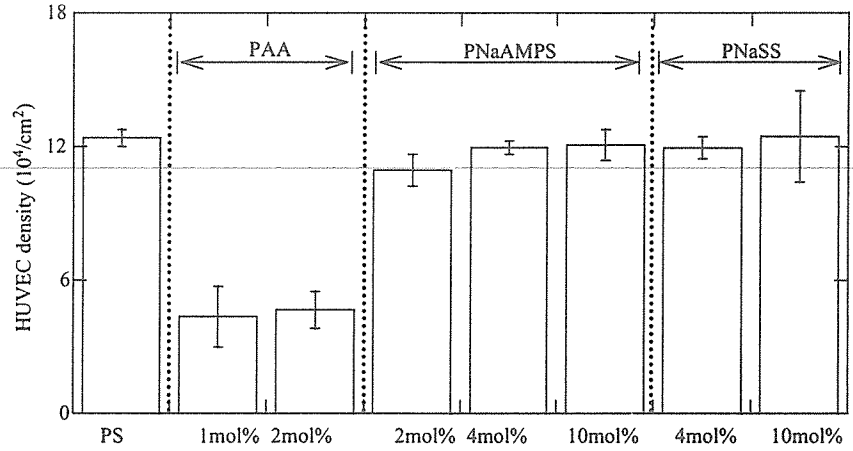


Fig. 3. Densities of the HUVECs that proliferate to confluent or sub-confluent on various kinds of scaffolds at 144 h. The numbers in the figures are the concentration of MBAA in molar ratio in relative to monomer used in gelation. Error ranges are standard deviations over $n = 4$–6 samples.

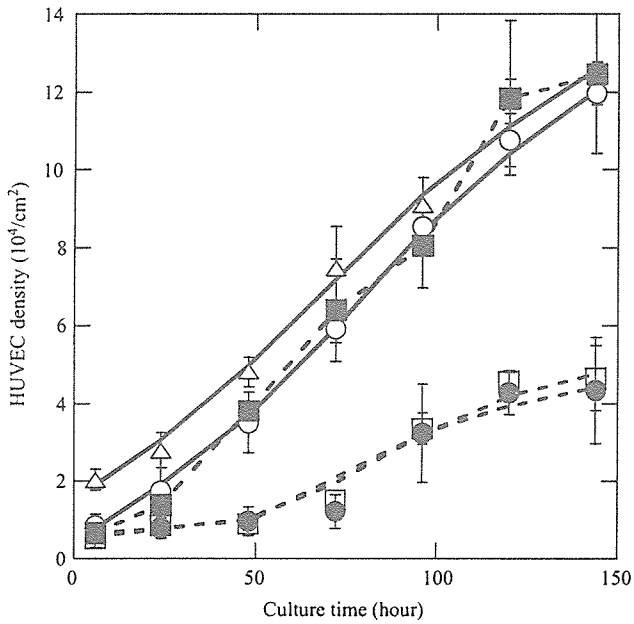


Fig. 4. Densities of the HUVECs cultured on various kinds of scaffolds as a function of culture time. (○) PNaAMPS (4 mol%), (■) PNaSS (10 mol%), (●) PAA (1 mol%), (□) PAA (2 mol%), (△) PS plate. Error ranges are standard deviations over $n = 4$–8 samples.

When the cross-linker concentration of PNaAMPS gel is 2, 4, and 10 mol%, the density of adhered platelets on the as-prepared HUVEC sheets is 183, 34, and 6 cells/$10^4$ μm$^2$, respectively. It shows that the platelet adhesion on the HUVEC sheets cultured on the strong anionic PNaAMPS gels decreases with increasing the cross-linker concentration of the gel.

It is a surprising result that no platelets adhere on the HUVEC sheets cultured on the PNaSS gels, regardless the cross-linker concentration (4 and 10 mol%) of the gel.

The above results demonstrated that the anti-platelet adhesion of the HUVECs cultured on various scaffolds increases in the order of PS < PAA < PNaAMPS < PNaSS, indicating that the platelet compatibility of the HUVECs cultured on these anionic gels is higher than that of PS plate. In addition, the ability of platelet adhesion on HUVECs depends on the chemical structure and cross-linker concentration of the gels used as scaffolds for HUVEC cultivation.

It was reported that EC glycocalyx relates to platelet adhesion [22,40]. We hypothesize that the glycocalyx, synthesized by HUVECs, is affected by the chemical and physical properties of the gels. To verify this, we modulated the glycocalyx on the cultured HUVECs, and studied its influence on the platelet compatibility.

The amount of glycocalyx is increased by a kind of cytokine, TGF-$\beta_1$, which promotes ECs to synthesize HSPGs, the main component of the PGs. It was demonstrated that TGF-$\beta_1$ treatment is able to increase more than 50% of HSPGs on EC surface. Furthermore, the glycolsaminoglycan chains of bioglycan synthesized by the ECs were elongated [23]. On the other hand, the amount of glycocalyx is decreased by a kind of enzyme, heparinase I, by cleaving glycolsaminoglycan side-chains from HSPGs [31–33]. It was demonstrated that heparinase treatments were able to reduce 27–51% fluorescence intensity of fluorescence-labeled wheat germ agglutinin [38], and reduce 45.9% of fluorescence intensity associated with heparin sulfate antibody [32].

Here, we use TGF-$\beta_1$ and heparinase I to treat the as-grown HUVECs and their adhesion to platelets were investigated. The SEM images of the adhered platelets on TGF-$\beta_1$ or heparinase I treated HUVECs cultured on various kinds of gels is shown in Fig. 7, the corresponding densities of adhered platelets on these samples are shown in Fig. 6. The morphology of adhered platelets on heparinase I treated HUVECs cultured on 1 mol% PAA gel was the same as that on 2 mol% PAA gel, and the morphology of adhered platelets on TGF-$\beta_1$ treated HUVECs cultured on 4 mol% PNaAMPS gel was the same as that on 2 mol% PNaAMPS gel (data are not shown).

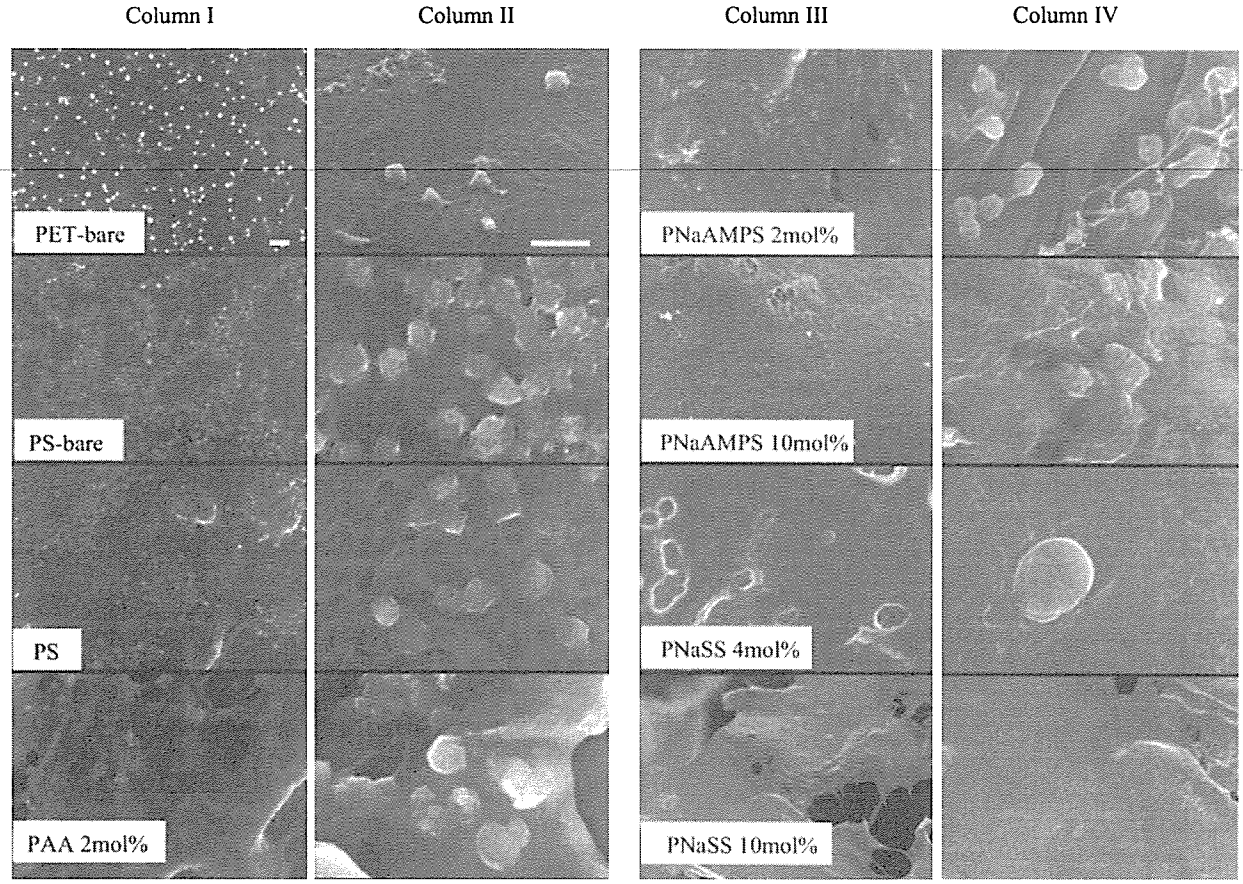


Fig. 5. SEM images of the adhered platelets on the HUVECs cultured on various kinds of substrates, and on bare PET and PS plates. The captions that have not 'bare' indicate the cultured HUVEC surface. Column II and IV is the magnified images of Column I and III, respectively. Scale bar: 5 μm.

Figs. 6 and 7 shows that by promoting the amount of HSPGs on HUVEC surface by TGF-$\beta_1$, the density of adhered platelets on the HUVECs cultured on PAA gel dramatically decreased from to 115 to 10 cells/$10^4$ μm$^2$. The density of adhered platelets on the HUVEC sheet cultured on PNaAMPS gel dramatically decreased from 183, 34 cells/$10^4$ μm$^2$ to 15, 17 cells/$10^4$ μm$^2$, respectively, for 2 and 4 mol% cross-linker concentration. The density of adhered platelets on the HUVEC sheet cultured on the 10 mol% PNaAMPS gel was 6 cells/$10^4$ μm$^2$, and it did not change by TGF-$\beta_1$ treatment. After treating the HUVECs with heparainase I that decreases the amount of the HSPGs, the density of adhered platelets on the HUVEC sheet cultured on PNaSS gel increased from 0 to 87 and 32 cells/$10^4$ μm$^2$, for 4 and 10 mol% cross-linker concentration, respectively.

We found that some platelets aggregate on the heparainase I treated HUVEC sheet cultured on 4 mol% PNaSS gel, while the adhered platelets on the as-prepared and TGF-$\beta_1$treated HUVECs are randomly distributed without aggregation (Fig. 7). Sibylle et al. reported that heparinase I induces platelets to expressed secretion maker (P-selectin) and aggregation maker (activated fibrinogen receptor GPIIb-IIIa) in vitro using whole blood flow cytometry [39]. About half of the adhered platelets aggregated on the heparainase I treated HUVEC sheet cultured on 4 mol% PNaSS gel was observed in our experiment, implying remained heparinase I on HUVEC sheet induces GPIIb-IIIa maker and further resulted to platelet aggregation. The effect of heparinase I on platelet aggregation and morphology in static conditions will be investigated in a future study.

The results show that for the cultured HUVECs that showed a large amount of platelets adhesion, after they were treated by TGF-$\beta_1$, platelet adhesion obviously decreased comparing with the as-prepared HUVECs. On the other hand, for the cultured HUVECs that did not induce platelet adhesion, after they were treated by heparinase I, platelets begun to adhere on the HUVECs. Therefore, the amount of glycocalyx on the cultured HUVECs modulates platelet adhesion. Our result is in agreement with the animal experiment that demonstrated the platelet adhesion is induced when the EC glycocalyx of vine of Golden hamsters is degraded by oxidized lipoproteins [40].

From the above results, we know that the HUVEC sheets cultured on the 4 and 10 mol% PNaSS gels, which did not induce platelet adhesion, have rich HSPGs on the cell surfaces. On the other hand, the HUVECs cultured on

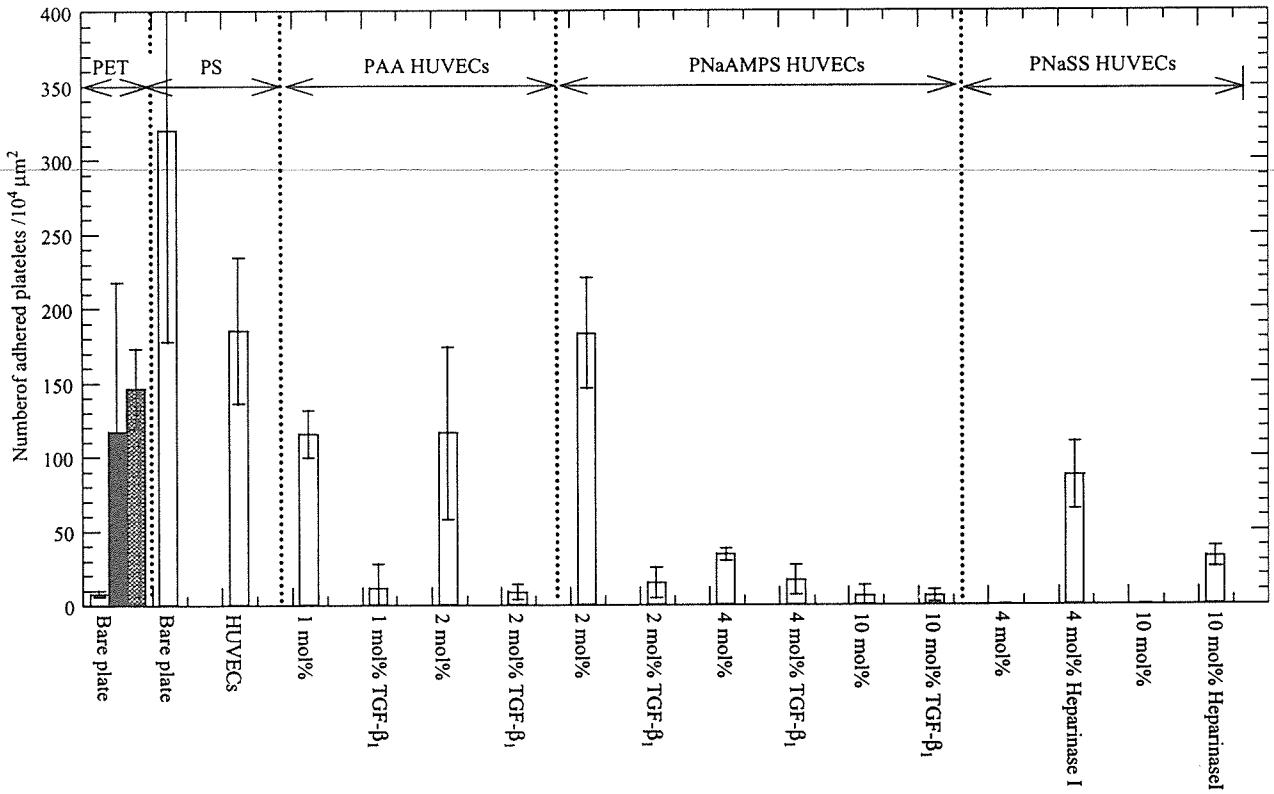


Fig. 6. Densities of adhered platelets on un-treated, TGF-$\beta_1$ treated, and heparinase I treated HUVECs cultured on various kinds of substrates, and on bare PET and PS plates. The numbers in the figures are the concentration of MBAA in molar ratio in relative to monomer used in gelation. White bar: normal platelet with spherical shape, black bar: round platelet with pseudopode extension, white bar with oblique lines: spreading platelet. Error ranges are standard deviations over $n = 3$–5 samples.

1 and 2 mol% PAA gels and 2 mol% PNaAMPS gels, which promoted a large amount of platelet adhesion, have poor HSPGs on the cell surfaces.

HajMohammadi et al. [41] reported that despite the reduction in heparin sulfate activity, the knockout mice failed to show accelerated thrombosis in the injured arteries compared with the wild-type counterparts. This finding raises the possibility that other glycosaminoglycans relate to platelet adhesion. Here, we have demonstrated that HSPGs are involve in platelet adhesion, but we do not exclude the possibility that other components of the glycocalyx, such as hyaluronic acid and chondroitin sulfate, influence platelet adhesion.

Our previous studies [42–44] showed that the freezing bound water in polymer is critical for inhibiting platelet adhesion. It suggested that sufficient amount of freezing bound water (a kind of crystallization water) prevents the blood components from direct contacting the polymer surface, which contributes to the excellent platelet compatibility. Some well-known biomaterials or polysaccharides [45–48], such as poly(ethylene glycol), gelatin, chitosan, and hyaluronic acid have freezing bound water. Our study suggested that HSPGs on the EC surface have crystallized water and the amount of crystallized water influences the blood compatibility of ECs. More detailed investigation about the state of water in glycocalyx will be undertaken in a separated study.

## 4. Conclusions

HUVECs can proliferate to sub-confluent or confluent on the negatively charged gels. However, not all the HUVECs cultured on the artificial scaffolds have platelet inhibition function even if they show the similar proliferation behavior. The study discoveres, for the first time to the authors' knowledge, that the HUVECs cultured on the PNaAMPS and PNaSS gels show excellent platelet compatibility, especially on the PNaSS gels. Furthermore, the platelet compatibility was enhanced when the HUVECs were treated with TGF-$\beta_1$, which stimulates synthesis of HSPGs on HUVECs surface, whereas the platelet compatibility was decreased when the HUVECs were treated with heparinase I, which disrupt HSPGs. These results indicate that the different platelet adhesion properties are attributed to the amount of glycocalyx on the HUVECs cultured on different kinds of gel scaffolds. These results demonstrate that it is possible to fabricate hybrid artificial blood vessel with high blood compatibility from PNaAMPS and PNaSS gels with ECs monolayer on their inner surfaces.

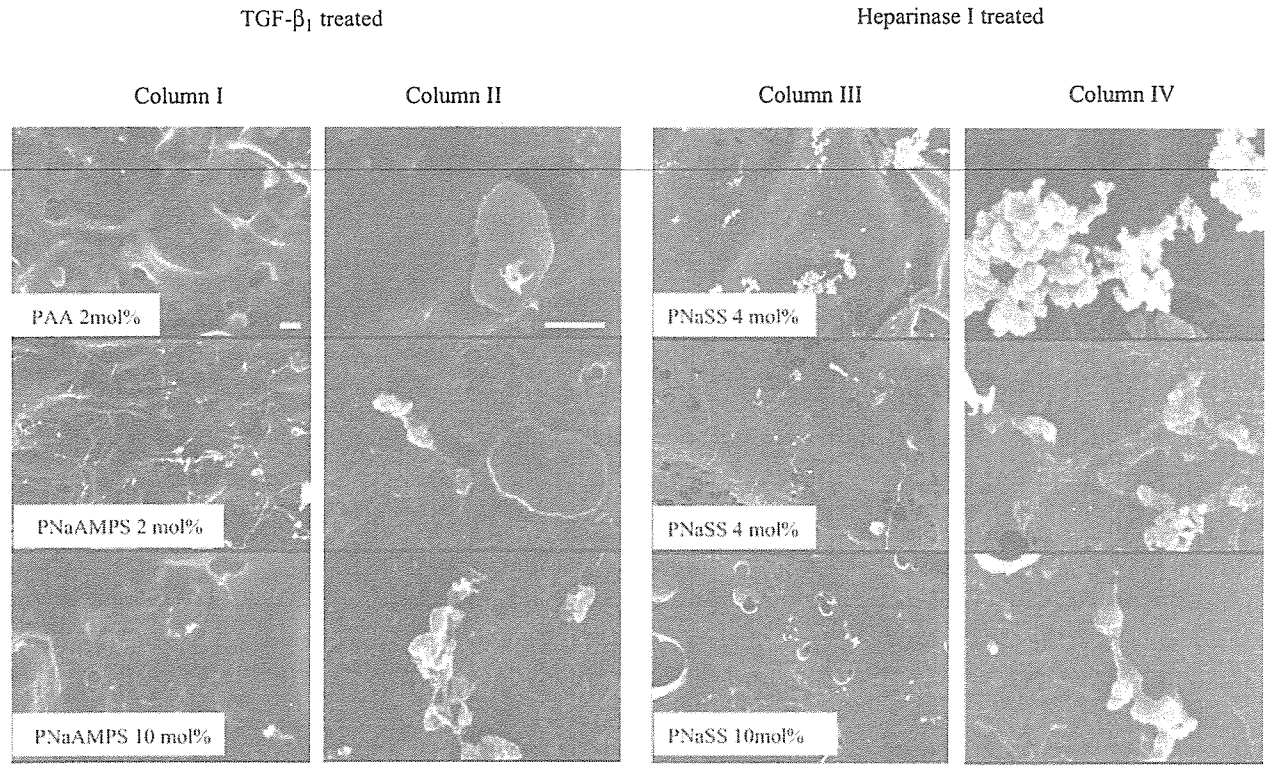


Fig. 7. SEM images of the adhered platelets on the HUVECs cultured on various kinds of gels treated by TGF-$\beta_1$ or heparinase I. Column II and IV is the magnified images of Column I and III, respectively. Scale bar: 5 μm.

## References


[1] Foley DP, Melkert R, Serruys PW. Influence of coronary vessel size on renarrowing process and late angiographic outcome after successful balloon angioplasty. Circulation 1994;90(3):1239–51.

[2] Harris JM. Poly(ethylene glycol) chemistry, biotechnical and biomedical applications. New York: Plenum Press; 1992.

[3] Tanaka M, Motomura T, Kawada M, Anzai T, Kasori Y, Shiroya T, et al. Blood compatible aspects of poly(2-methoxyethylacrylate) (PMEA)—relationship between protein adsorption and platelet adhesion on PMEA surface. Biomaterials 2000;21:1471–81.

[4] Tanaka M, Motomura T, Kawada M, Anzai T, Kasori Y, Shimura K, et al. A new bloodcompatible surface prepared by poly(2-methoxyethylacrylate) (PMEA) coating—protein adsorption on PMEA surface. Jpn J Artif Organs 2000;29:209–16.

[5] Tsuruta T. Contemporary topics in polymeric materials for biomedical applications. Adv Polym Sci 1996;126:1–51.

[6] Severian D. Polymeric biomaterials. New York: Mercel Dekker, Inc.; 2002.

[7] Okano T, Nishiyama S, Shinohara I, Akaike T, Sakurai Y, Kataoka K, et al. Effect of hydrophilic and hydrophobic microdomains on mode of interaction between block copolymer and blob platelets. J Biomed Mater Res 1981;15:393–403.

[8] Losia P, Lombardib S, Brigantia E, Soldania G. Luminal surface microgeometry affects platelet adhesion in small-diameter synthetic grafts. Biomaterials 2004;25:4447–55.

[9] Brinkman E, Foot A, Does L, Bantjes A. Platelet deposition studies on copolyether urethanes modified with poly(ethylene oxide). Biomaterials 1990;3:200–5.

[10] Mori Y, Nagaoka S, Takiguchi T, Kikuchi T, Noguchi N, Tanzawa H, et al. A new antithrombogenic material with long polyethylene oxide chain. Trans Am Soc Artif Intern Organs 1982;28: 459–63.

[11] Haimovich H, Difazio L, Katz D, Zhang L, Greco RS, Dror Y, et al. A new method for membrane construction on ePTFE vascular grafts: effect on surface morphology and platelet adhesion. J Appl Polymer Sci 1997;63:1393–400.

[12] Lee JH, Khang G, Lee JW, Lee HB. Platelet adhesion onto chargeable functional group gradient surfaces. Int J Biol Macromol 2003;32:17–22.

[13] Park JH, Park KD, Bae YH. PDMS-based polyurethanes with MPEG grafts: synthesis, characterization and platelet adhesion study. Biomaterials 1999;20:943–53.

[14] Zhang J, Yuana J, Yuan Y, Zang X, Shena J, Lin S. Platelet adhesive resistance of segmented polyurethane film surface grafted with vinyl benzyl sulfo monomer of ammonium zwitterions. Biomaterials 2003; 24:4223–31.

[15] Fujimoto K, Tadokoro H, Ueda Y, Ikada Y. Polyurethane surface modification by graft polymerization of acrylamide for reduced protein adsorption and platelet adhesion. Biomaterials 1993;14:442–8.

[16] Van den Beng B, Vink H, Spaan JA. The endothelial glycocalyx protects against myocardial edema. Circ Res 2003;92:592–4.

[17] Yanagishita M, Hascall VC. Cell surface heparan sulfate proteoglycans. J Biol Chem 1992;267:9451–4.

[18] Hallgren J, Spillmann D, Pejler G. Structural requirements and mechanism for heparin-induced activation of a recombinant mouse mast cell tryptase, mouse mast cell protease-6. J Biol Chem 2001;276: 42774–81.

[19] Weitz JI. Heparan sulfate: antithrombic or not? J Clin Invest 2003; 111:952–4.

[20] Nugent MA, Nugent HM, Iozzoi RV, Sanchack K, Edelman ER. Perlecan is required to inhibit thrombosis after deep vascular injury and contributes to endothelialcell-mediated inhibition of intimal hyperplasia. PNAS 2000;97:6722–7.

[21] Segev A, Nili N, Strauss BH. The role of perlecan in arterial injury and angiogenesis. Cardiovasc Res 2004;63:603–10.

[22] Guyton JR, Rosenberg RD, Clowes AW, Karnovsky MJ. Inhibition of rate arterial smooth muscle cell proliferation by heparin. In vivo studies with anticoagulant and nonanticoagulant heparin. Circ Res 1980;46:625–34.
[23] Kaji T, Yamada A, Miyajima S, Yamamoto C, Fujiwara Y, Wight TN, et al. Cell density-dependent regulation of proteoglycan synthesis by transforming growth factor-$\beta_1$ in cultured bovine aortic endothelial cells. J Biol Chem 2000;275:1463–70.
[24] Pries AR, Secomb TW, Jacobs H. Microvascular blood flow resistance: role of endothelial surface layer. Am J Physiol 1997;273: H2272–9.
[25] Woodsa AM, Rodenberga EJ, Hilesb MC, Pavalkoa FM. Improved biocompatibility of small intestinal submucosa (SIS) following conditioning by human endothelial cells. Biomaterials 2004;25:515–5.
[26] Chen YM, Tanaka M, Gong JP, Yasuda K, Yamamoto S, Shimomura M, et al. Biomaterials used for artificial blood vessels. JP Patent no.2006-141838
[27] Lee KY, Mooney DJ. Hydrogels for tissue engineering. Chem Rev 2001;10:1869–79.
[28] Hoffman AS. Hydrogels for biomedical applications. Adv Drug Del Rev 2002;54:3–12.
[29] Chen YM, Shiraishi N, Satokawa H, Kakugo A, Narita T, Gong JP, et al. Cultivation of endothelial cells on adhesive protein-free synthetic polymer gels. Biomaterials 2005;26:4588–96.
[30] Kasinath BS. Glomerular EC proteoglycan regulation by TGF-$\beta_1$. Arch Biochem Biophys 1993;305:370–7.
[31] Linhardt RJ, Turnbull JE, Wang HM, Loganathan D, Gallagher JT. Examination of the substrate specificity of heparin and heparan sulfate lyases. Biochemistry 1990;29:2611–7.
[32] Florian JA, Kosky JR, Ainslie K, Pang Z, Dull RO, Tarbell JM. Heparan sulfate proteoglycan is a mechanosensor on endothelial cells. Circ Res 2003;93:e136–42.
[33] Mulivor AW, Lipowsky HH. Role of glycocalyx in leukocyte-endothelial cell adhesion. Am J Physiol Heart Circ Physiol 2002;283: H1282–91.
[34] Park JH, Bae YH. Hydrogels based on poly(ethylene oxide) and poly(tetramethylene oxide) or poly(dimethyl siloxane): synthesis, characterization, in vitro protein adsorption and platelet adhesion. Biomaterials 2002;23:1797–808.
[35] Zhu A, Chen T. Blood compatibility of surface-engineered poly (ethylene terephthalate) via *o*-carboxymethylchitosan. Coll Surf B: Biointerfaces 2006;50:120–5.
[36] Gappa-Fahlenkamp H, Lewis R S. Improved hemocompatibility of poly(ethylene terephthalate) modified with various thiol-containing groups. Biomaterials 2005;26:3479–85.
[37] Brockstedt U, Dobra K, Nurminen M, Hjerpe. Immunoreactivity to cell surface syndecans in cytoplasm and nucleus: tubulin-dependent rearrangements. Exp Cell Res 2002;274:235–45.
[38] Haldenby KA, Chappel DC, Winlove CP, Parker KH, Firth JA. Focal and region variations in the composition of glycocalyx of large vessel endothelial. J Vasc Res 1994;31:2–9.
[39] Kozek-Langenecker SA, Mohammad SF, Masaki T, Kamerath C, Cheung AK. The effects of heparin, protamine, and heparinase 1 on platelets in vitro using whole blood flow cytometry. Anesth Analg 2000;90:808–12.
[40] Vink H, Constantinescu AA, Spaan JAE. Oxidize lipoproteins degrade the endothelial surface layer implications for platelet-endothelial cell adhesion. Circulation 2000;101:1500–2.
[41] HajMohammadi S, Enjyoji K, Princivalle M, Christi P, Lech M, Beeler D, et al. Normal levels of anticoagulant heparan sulfate are not essential for normal hemostasis. J Clin Invest 2003;111:989–99.
[42] Tanaka M, Mochizuki A. Effect of water structure on blood compatibility—thermal analysis of water in poly(meth)acrylate. J Biomed Mater Res 2004;68A:684–95.
[43] Tanaka M, Mochizuki A, Ishii N, Motomura T, Hatakeyama T. Study of blood compatibility with poly(2-methoxyethyl acrylate). Relationship between water structure and platelet compatibility in poly(2-methoxyethyl acrylate-*co*-2-hyydroxyethylmeth acrylate). Biomacromolecules 2002;3:36–41.
[44] Tanak M, Motomura T, Ishii N, Shimura K, Onishi M, Mochizuki A, et al. Cold crystallization of water in hydrated poly(2-methoxyethyl acrylate) (PMEA). Polym Int 2000;49:1709–13.
[45] Hatakeyama H, Hatakeyama T. Interaction between water and hydrophilic polymers. Thermochim Acta 1995;308:3–22.
[46] Graham NB, Zulfiqar M, Nwachuku NE, Rashid A. Interaction of poly(ethylene oxide) with solvents: 2. Water-poly(ethylene glycol). Polymer 1989;30:528–33.
[47] Ratto J, Hatakeyama T, Blumstein RB. Differential scanning calorimetry investigation of phase transitions in water/chitosan systems. Polymer 1995;36:2915–9.
[48] Nishinari K, Watase M, Hatakeyama T. Effects of polyols and sugars on the structure of water in concentrated gelatin gels as studied by low temperature differential scanning calorimetry. Coll Polym Sci 1997;275:1078–82.

COLLOIDS AND SURFACES
A: PHYSICOCHEMICAL AND ENGINEERING ASPECTS

Volumes 284+285 (2006)

# Simple preparation of hemispherical polystyrene particles

Takeshi Higuchi [a], Hiroshi Yabu [b,c], Masatsugu Shimomura [b,c,d,*]

[a] *Graduate School of Science, Hokkaido University, N10W8, Kita-ku, Sapporo, Hokkaido 060-0810, Japan*
[b] *Nanotechnology Research Center, Research Institute for Electronic Science, Hokkaido University, N21W10, Kita-ku, Sapporo, Hokkaido 001-0021, Japan*
[c] *Frontier Research System, The Institute of Physical and Chemical Research (RIKEN), 2-1 Hirosawa, Wako, Saitama 351-0198, Japan*
[d] *Core Research for Evolutional Science and Technology (CREST), Japan Science and Technology Agency (JST), 4-1-8 Honcho, Kawaguchi, Saitama 332-0012, Japan*

Received 1 August 2005; received in revised form 17 October 2005; accepted 28 October 2005
Available online 4 January 2006


ELSEVIER

Amsterdam – Boston – Jena – London – New York – Oxford – Paris – Philadelphia – San Diego – St. Louis